Polymer

One-Step Nanomorphology Control of Self-Organized Projection Coronas in Uniform Polymeric Nanoparticles†

Kazuhiro Hamada,[a] Tatsuo Kaneko,[a,c] Ming Qing Chen,[b] Mitsuru Akashi[a,c]*

a) Department of Applied Chemistry, Graduate School of Engineering, Osaka University, 2-1 Yamada-oka, Suita 565-0871, Japan

b) School of Chemical and Material Engineering, Southern Yangtze University, Wuxi 214036, P. R. China

c) Core Research for Evolutional Science and Technology (CREST), Japan Science and Technology Agency (JST), Tokyo

**Correspondence author: akashi@chem.eng.osaka-u.ac.jp*

TEL: +81-6-6879-7357 FAX: +81-6-6879-7359

Abstract

Uniform polymeric nanoparticles with various morphologies of projection coronas like the viruses in the coronavirus group have been formed by the self-organization of macromolecular chains polymerizing in a dispersion system of styrene (St), acrylonitrile (AN) and poly(ethylene glycol) monomethacrylate (PEGm) in a polar solvent (water/ethanol). An increase in the water composition reduced the crystallization degree of AN units, resulting in a variety of the nanoparticle morphology such as the increased particle size, the reduced projection size, the increased projection number, and the decreased inter-projection distance. The difference in the projection morphology strongly affected a dispersibility in water.

Keywords:

1. Polymeric nanoparticles 2. Patterned crystallization 3. Morphology control

1. Introduction

Polymeric particles of nano- and micro-scale have an extremely large specific surface area giving an excellent material sorbability, which attracts broad attention in the fields of drug delivery,[1,2] chromatography and catalyst.[3] The morphological control of particles is one method for creating new functions and improving the performance of polymeric nanoparticles. Since it is expected that non-spherical nanoparticles can have a larger specific area and higher material sorbability than nanospheres of equal size, particles of various morphologies, such as raspberry-like,[4,5]

snowman-like,[6,7] and virus-like[8,9] have been prepared by multistep preparation techniques such as hetero aggregation[8,9] and seed polymerization.[4-7]

In our previous works, polymeric nanoparticles on which nano-projections were uniformly distributed over the whole surface have been prepared using one-step preparation by a dispersion radical copolymerization of styrene, acrylonitrile and poly(ethylene glycol) monomethacrylate.[10] A similarity to the virus arises since these nanoparticles are formed by the self-organization of the macromolecular chains. Another similarity is based on the morphology. Tomato bushy stunt virus has a diameter of 33nm and 90 projections with a length of 3nm on the surface,[11] while the viruses in coronavirus group has a diameter range 75-160nm and many projections with a length range 12-14nm.[12] Most viruses have the projections with a bigger or smaller size on the surface to a greater or less extent; the viruses have a variety of projection morphology in terms of the size, the number, and the inter-projection distance, showing individual living characteristics. On the other hand, the morphology and number density of projection coronas of the present synthetic nanoparticles have never been controlled although the growth of the projections was observed by a change in the polymerization time.[13] In this paper, we aim to give a variety of the morphology of the nanoparticle by controlling the particle size, the projection size, the projection number, and the inter-projection spacing. We find that the morphology is successfully controlled by changing the solvent for self-organization, and the morphology control is very effective on the water-dispersibility of the nanoparticles.

2. Experimental Section

2.1. Materials

Styrene (St; WAKO Pure Chemical Ind. Ltb.) and acrylonitrile (AN; WAKO Pure Chemical Ind. Ltd.) which were used as monomers were distilled in vacuo just before use. Poly(ethylene glycol) monomethacrylate (PEGm; number average molecular weight M_n = 1740) donated from Nippon Oil and Fats Co. was used as received. 2,2'-Azobis(isobutyronitorile) (AIBN; WAKO Pure Chemical Ind. Ltd.) which was used as a radical initiator was recrystallized from ethanol (WAKO Pure Chemical Ind. Ltb) before use. A mixture of distilled water and ethanol was used as the polymerization medium.

2.2. Polymerization

Dispersion polymerization of St, AN, and PEGm were carried out batchwise in a glass tube. The general procedure used to prepare all of the nanoparticles was as follow: St (0.9 mmol), AN (3.0 mmol), PEGm (0.027 mmol; 0.7 mol% to St and AN), and AIBN (1 mol% of total monomers) were added to the ethanol/water (= 0/100, 10/90, 20/80, 30/70, 40/60, 50/50, 60/40, 70/30, 80/20, 90/10, 100/0 (v/v)) mixture (Table 1). Each polymerization batch was prepared in a glass tube and was repeatedly degassed by freeze-thaw cycles in a vacuum apparatus, sealed off, and then placed in an incubator at 60 ^{o}C for 24h. The resulting solutions were dialyzed in ethanol and distilled deionized water using a cellulose doalyzer tube to remove unreacted monomer. The ratex particles were then centrifugated and redispersed in water.

2.3. Measurements

Scanning electron microscopy (SEM) images were obtained with a JSM-6700F microscopic operated at an acceleration voltage of 3.0 kV. Specimens were prepared by

slow evaporation of a drop of approximately diluted solution deposited onto a brass stage followed by osmium spattering.

Transmission electron microscopy (TEM) images were obtained with a Hitachi H-700H microscopic operated at an acceleration voltage of 150 kV at a magnification of 60 000x. Specimens were prepared by slow evaporation of a drop of approximately diluted solution deposited onto a collodion-coated copper mesh grid followed by carbon spattering.

Dynamic Light Scattering (DLS) measurement was performed with a BECKMAN COULTER Laser Diffraction Particle Size Analyzer LS 13-320.

Viscosity measurement was performed on PEG solution at a temperature of 30°C by means of standard Ostwald viscometers. Before measuring viscosity, the samples were stabilized for sufficient time at the given temperature.

Electron spectroscopy for chemical analysis (ESCA) was performed with a Shimadzu ESCA 1000 apparatus employing Mg Kα radiation (1253.6 eV) and a pass energy of 31.5 eV. The higher resolution utility scans were used to determine the atomic concentrations of carbon, nitrogen, and oxygen.

X-ray diffraction patterns were taken with a RIGAKU X-ray generator (ultraX 18; thin-film out-of-plain system) emitting Ni-filered Cu Kα radiation (40 kV, 200 mA) at scanning angles ranging from 40^{o} to 5^{o} at a scanning rate of 3^{o} min^{-1}.

3. Results and Discussion

The terpolymers were synthesized by dispersion copolymerization of St, AN, and PEGm (number-average molecular weight M_n = 1740) in the presence of AIBN (radical initiator) in a water/ethanol mixed solvent with various compositions at 60 °C

for 24h (Scheme 1 and Table 1). The reaction solution was transparent in the early stages but became cloudy with the progress of polymerization in the water composition range 10-50 vol%. On the other hand, the reaction solution was cloudy before polymerization in a water composition range of more than 60% presumably due to the poor solvent affinity of the St monomer and AN monomer.

Figure 1 shows scanning electron microscopy (SEM) images of the nanoparticles. When the water composition was 0 vol% and 10 vol%, nanoparticles with projection coronas were not formed (not shown). As shown in Figure 1a, nanoparticles prepared in the solvent with a water composition of 20 vol% had projection coronas similar to a coronavirus in morphology. In solvent compositions of 30, 40, and 50 vol%, projection coronas were also confirmed distinctly (Figure 1b, 1c, 1d). However, this kind of nanoparticle morphology was not formed when polymerization was performed in a water composition of more than 60 vol%. This may be due to a difference in the polymerization system; the dispersion system is indispensable for projection formation. When the water composition increased, the particle morphology changed. The effects of water composition on particle morphology are shown in Figure 2 - 4.

Figure 2 shows the particle size measured by dynamic light scattering (DLS), which is close to that estimated from the SEM images. The particle size increased with an increase in water composition. The same phenomenon was observed in the nanoparticles composed of St and PEGm.[14] The hydrophobic St formed a larger nanoparticle core under conditions of higher water content.

Figure 3 shows the average volume of a projection (V_p) calculated from Figure 1 using an image data processing tool (Win ROOF) based on the assumption of a hemispherical projection; the average number of projections (n) on a particle was also

counted. When the water composition was 20 vol%, V_p was 7.2×10^4 nm^3 which was about 3% of the particle volume, V. Increasing the water composition decreases V_p and increases V, and V_p became about 0.1 % of V. When the water composition was 20 vol%, n was 26 which increased up to 65 with an increase in water composition.

Figure 4 shows the average inter-projection distance (d) and the specific surface area (S) of the nanoparticles. d was measured directly from the SEM images. When the water composition was 20 vol%, d was 95 nm; d decreased down to 45 nm with an increase in the water composition. Figure 3 and Figure 4 show that a larger number of smaller projections appeared on the nanoparticle surface with a higher water composition. When the water composition was 20 vol%, S was 1.73×10^{-2} nm^2/nm^3 which increased to 2.18×10^{-2} nm^2/nm^3 with an increase in water composition. Consequently, S was controlled by a change in solvent composition and S then was about two times larger than that of nanospheres of equal size. Validity of all the calculated values were confirmed by recalculation using transmission electron microscopic images (not shown).

Since the projection morphology may be related to the solvent affinity of the particle surface, i.e. PEG chains, we investigated the solvent affinity of PEG in terms of reduced viscosity behavior. Figure 5 shows changes in the reduced viscosity as a function of the water composition. PEG with a molecular weight of 10000 was used as a sample because a polymer chain with a larger molecular weight shows a larger change in reduced viscosity by a conformation change. The reduced viscosity increased with increasing water composition showing that the PEG chain took an extended conformation because of increased solvent affinity when the water composition

increased. This finding suggests that PEGm graft chains existing on the nanoparticle surface take an extended conformation in a high water composition environment.

Elemental analysis on the surface of the nanoparticles was performed by X-ray photoelectron spectroscopy (XPS). We show O/C and N/C on the surface of the particles prepared under different water compositions together with the bulk composition of AN units to the total units in Figure 6. The O/C ratio slightly decreased with an increase in water composition while the N/C ratio increased. This result shows that the amount of AN increased on the particle surface as the water composition increased in spite of a decrease in the bulk composition from 57.6 to 47.3unit mol%. This phenomenon indicated the excess surface accumulation of AN units, which may be associated with the fact that PAN has some solubility in water/ethanol solvent.[15] Since the number of projections also increased, we can support the previously-proposed hypothesis that the projection was mainly comprised of AN.[13] The slight decrease in O/C may result from a decrease in the relative amount of PEG to AN units.

We previously hypothesized that the projection formed on the particle surface was caused by the crystal growth of AN. Using the present samples with various morphologies, we attempted to investigate the relathionship between the nanoparticles crystallinity and the projection size. The main peak of the crystal of PAN is detected in $2\theta = 17.1^{o}$ (200) according to the literature.[16] Figure 7a shows XRD patterns of the nanoparticles showing a sharp peak at $2\theta = 17.1^{o}$ (θ; diffraction angle) and large amorphous peak at around 23^{o}. Crystallization degree of AN units to total nanoparticles were shown as a function of the projection volume in Figure 7b. The crystallinity of nanoparticle linearly increased with a increase in projection volume. As a concequence, the projection on the particle surface can be formed by the crystal growth of AN units.

Based on these results, we discussed the reason for the change in the arrangement of projection coronas on the nanoparticles. We previously proposed a hierarchical structure for the nanoparticles with projection coronas: PEG grafts exist on an AN-rich shell covering the St-rich core.[13] Since the nanoparticle created from St and PEGm formed no projections, AN is indispensable in the formation of projection coronas.[13] Since PAN has some solubility in water/ethanol solvent,[15] PAN chains having PEGm grafts may be capable of solvating. The shell in PAN and PEGm may be swollen in solvent with connecting to a PSt core. According to a previous study, the morphology was spherical at the beginning of polymerization, and the projection grew with polymerization time but the number of projections was constant regardless of polymerization time.[13] Namely, the number of projections is determined at the early stages of projection formation where PEGm chains first stick out from the shell dragging out PAN units with them. In this case, the solvent affinity of a PEGm may be an important factor for projection formation. If the water composition is higher, a larger number of AN units exist on the particle surface (Figure 6) in the presence of better-solvated PEGm chain yielding a larger number of projection nuclei. The solvation can give a chain mobility to make a crystallization of AN units and the projection is formed. If the AN composition is high, the crystal growth happens in a lot of parts because a number of crystal nuclei were formed on the particle surface. The higher projection population might make its size (Figure 8). Thus, solvent affinity is a crucial factor in controlling particle morphology.

Finally we investigated the relationship between the nanoparticle morphology and the water-dispersibility. Although the phenomenon that the smaller nanoparticles have the higher water-dispersibility was widely-confirmed, the effects of their morphology

were never investigated as far as we know. We performed a simple test of the water-dispersibility of the present nanoparticles; after the water-dispersion solutions of the nanoparticles (1mg/ml) whose morphologies are shown in Figure 1a-d were centrifuged at 9000 rpm for one minute at 20^{o}C, their opaqueness was observed. Figure 9 shows the representative photograph of the dispersions (The morphology of right side and left side was shown in Figure 1a and 1d, respectively) after the centrifugation. While the nanoparticles with the smallest particle size and the largest projections whose morphology is shown in Figure 1a was precipitated, the nanoparticles with the largest particle size and the smallest projections (Figure 1d) kept the water-dispersibility well. The water-dispersibility increased with increasing the particle size, contrarily to the widely-confirmed phenomenon in this size range of 50nm ~ 10μm. In the present case, the projection morphology may affect the water-dispersibility more effectively rather than the particle size. The increase in the number of the projection with the reduced size increased S, which should strongly enhance the water-dispersibility of the nanoparticles.

4. Conclusion

In summary, the morphology of nanoparticles, on which nano-projections were distributed over the entire surface prepared by a dispersion copolymerization of AN, St, and PEGm in water/ethanol mixed solvent was successfully controlled by changing the solvent composition. When the water composition was increased up to 50 vol% to total solvent volume, the particle size increased, the projection size decreased, the number of projections increased, and the spacing between projections decreased. On the other hand, nanoparticles with projection coronas were not formed when the water composition was

higher than 50 vol% since the dispersion system was not created during polymerization. The morphology control was based on the solvent affinity of PEGm graft chains, which extended better in higher water compositions and concentrate the AN units in the shell layer to form larger amount of crystalline projections. The ratio of the specific surface area to the particle volume was from 1.7×10^{-2} nm^2/nm^3 to 2.2×10^{-2} nm^2/nm^3, which is twice as large as that of nanospheres of equal size. The increased number of the projection with the reduced size was effective on increasing the water-dispersibility of the nanoparticles. As a result, we prepared the nanoparticles with various morphologies similar with the viruses in the coronavirus group. The study is currently continuing to investigate the morphology-specific catch-up behavior of the nano-sized materials such as viruses using the inter-projection gap on the nanospheres.

Acknowledgment

This research was partly supported by a Grant-in-Aid for Tokuyama Science Foundation. We show an appreciation to Mr. Kakoi, a technician of Kagoshima University, and Dr. Okunishi of JEOL for TEM studies, and Mr. Ohzono a technician of Kagoshima University for XPS studies.

References

† This paper is part 39 in the series of the study on Graft Copolymers Having Hydrophobic Backbone and Hydrophilic Branches.

[1] Akagi T, Kawamura M, Ueno M, Hiraishi K, Adachi M. Serizawa T, Akashi, M, Baba M. J. Med. Virol. 2003; 69: 163.

[2] Rihova B. Adv. Drug Delivery. Rev. 2002**;** 54: 653.

[3] Chen CW, Serizawa T, Akashi M. Chem. Mater. 2002**;** 14: 2232.

[4] Reculusa S, Poncet-Legrand C, Ravaine S, Mingotaud C, Duguet E, Bourgeat-Lami E. Chem. Mater. 2002**;** 14: 2354.

[5] Hölderle M, Bruch M, Lüchow H, Gronski W, Mülhaupt R. J. Polym. Sci. Part A: Polym. Chem. 1998**;** 36: 1821.

[6] Okubo M, Yamashita T, Minami H, Konishi Y. Colloid Polym. Sci. 1998**;** 276: 887.

[7] Okubo M, Wang Z, Yamashita T, Ise E, Minami H. J. Polym. Sci. Part A: Polym. Chem. 2001**;** 39: 3106.

[8] Dubois M, Demé B, Gulik-Krzywicki T, Dedieu JC, Vautrin C, Désert S, Perez E, Zemb T. Nature 2001**;** 411: 672.

[9] Hubert H, Devouard B, Garvie LAJ, O'Keeffe M, Buseck PR, Petuskey WT, McMillan P F. Nature 1998; 391: 376.

[10] Chen MQ, Kaneko T, Chen CH, Akashi M. Chem. Lett. 2001; 1306.

[11] Branden C, Tooze J. Introduction to Protein Structure Second Edition (1999), Taylor & Francis, New York.

[12] Matthews REF. Classification and Nomenclature of Viruses. Fourth Report of the International Committee on Taxonomy of Viruses. (1982) S. Karger AG, Basel.

[13] Kaneko T, Hamada K, Chen MQ, Akashi M. *Macromolecules* 2004**;** 37: 501.

[14] Chen MQ, Serizawa T, Kishida A, Akashi M. J. Polym. Sci. Part A: Polym. Chem. 1999**;** 37: 2155.

[15] Brandrup J, Immergut EH. POLYMER HANDBOOK THIRD EDITION (1989), VII/385.

[16] Minagawa M, Taira T, Yabuta Y, Nozaki K, Yoshii F. Macromolecules. 2001, 34,

3679.

Figure captions

Scheme 1. Molecular structure of poly{styrene-*co*-acrylonitrile-*co*-poly(ethylene glycol) monomethacrylate}.

Figure 1. Scanning electron microscopy images of nanoparticles of poly{styrene-*co*-acrylonitrile-*co*- poly(ethylene glycol) monomethacrylate}. **a**. water composition = 20 vol%, **b**. water composition = 30 vol%, **c**. water composition = 40 vol%, **d**. water composition = 50 vol%.

Figure 2. The effects of water composition in a polymerization solvent ethanol/water (5ml) on the particle size.

Figure 3. The effects of water composition in a polymerization solvent ethanol/water (5ml) on the average projection volume (○) and average number of projections (□).

Figure 4. The effects of water composition in a polymerization solvent ethanol/water (5ml) on the average distance between the projections (○) and the specific surface area (□).

Figure 5. The effects of water composition in a polymerization solvent ethanol/water (5 ml) on the reduced viscosity of the poly(ethylene glycol) (M_n: 10000).

Figure 6. Solvent composition dependence of the elemental composition of the nanoparticle surface of poly{styrene-*co*-acrylonitrile-*co*-poly(ethylene glycol) monomethacrylate} (○) O/C, (□) N/C (left axis) and of the bulk composition of acrylonitrile units(■) (right axis).

Figure 7. a) XRD patterns of poly{styrene-*co*-acrylonitrile-*co*-poly(ethylene glycol) monomethacrylate} prepared with water compositions of 20 ($V_p = 7.19 \times 10^4$ nm^3), 30 ($V_p = 4.98 \times 10^4$ nm^3), 40 ($V_p = 2.15 \times 10^4$ nm^3), and 50% ($V_p = 1.12 \times 10^4$ nm^3). b) Relation ship between crystalline degree AN units and projection volume, V_p.

Figure 8. Schematic illustration of the shape change mechanism f the nanoparticles with projection coronas composed of poly{styrene-*co*-acrylonitrile-*co*-poly(ethylene glycol) monomethacrylate}.

Figure 9. Water-dispersion behavior for the nanoparticles of poly{styrene-*co*-acrylonitrile-*co*-poly(ethylene glycol) monomethacrylate} after centrifugation (9000rpm for 1min, 20°C) ; (right) The nanoparticles prepared in the solvent with a water composition of 20 vol%. The morphology was shown in Figure 1a, (left) The nanoparticles prepared in the solvent with a water composition of 50 vol%. The morphology was shown in Figure 1d.

Table(s)

Click here to download high resolution image

Table 1. Synthesis and Characterization of Poly(St-*co*-AN-*co*-PEGm) with Various Solvent Compositions[a)]

Run	PEGm M_n	PEGm (mmol)	St (mmol)	AN (mmol)	Solvent water/ethanol = (v/v)	Composition ratio St : An : PEGm (%)
1	1740	0.027	0.9	3.0	10/90	41.5 : 58.2 : 0.3
2	1740	0.027	0.9	3.0	20/80	42.1 : 57.6 : 0.3
3	1740	0.027	0.9	3.0	30/70	45.8 : 53.9 : 0.3
4	1740	0.027	0.9	3.0	40/60	49.5 : 50.3 : 0.2
5	1740	0.027	0.9	3.0	50/50	52.5 : 47.3 : 0.2
6	1740	0.027	0.9	3.0	60/40	53.0 : 46.9 : 0.1

[a)]The polymerization was carried out in the solvent (5ml) at 60°C for 24h.

Table 1 Hamada et al.

Figure(s)

Click here to download high resolution image

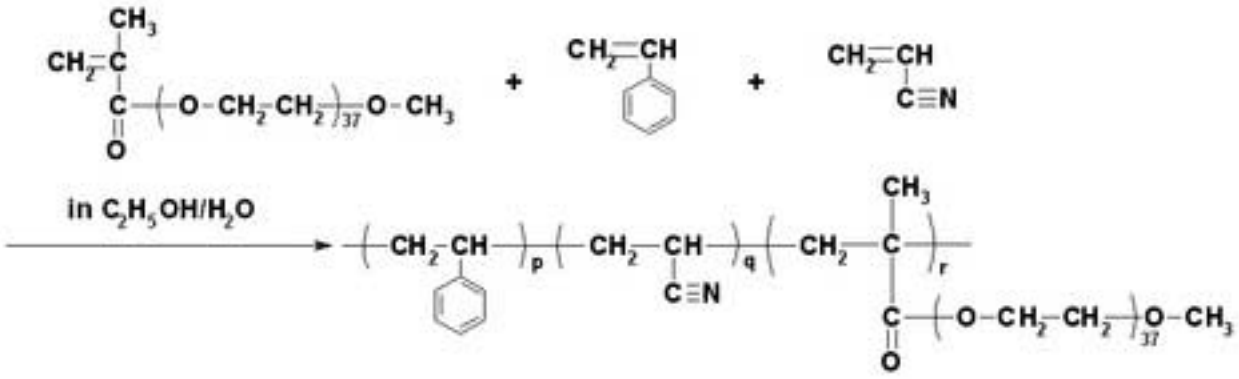

Scheme 1 Hamada et al.

Figure(s)
Click here to download high resolution image

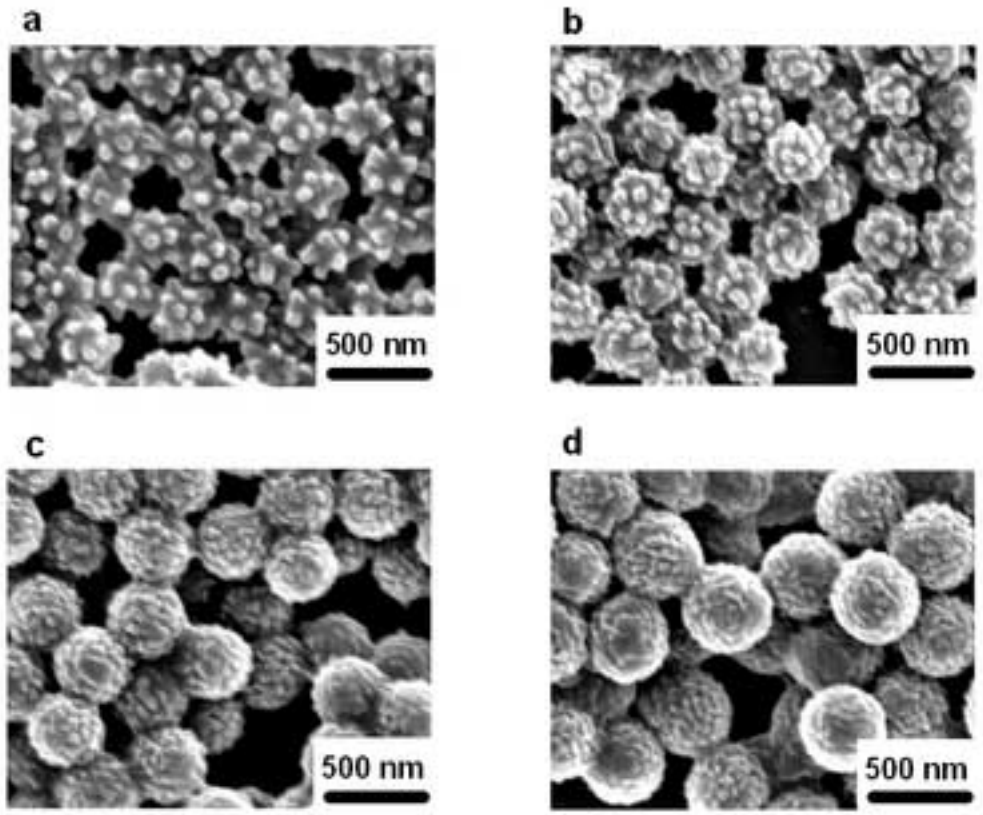

Figure 1 Hamada et al.

Figure(s)

Click here to download high resolution image

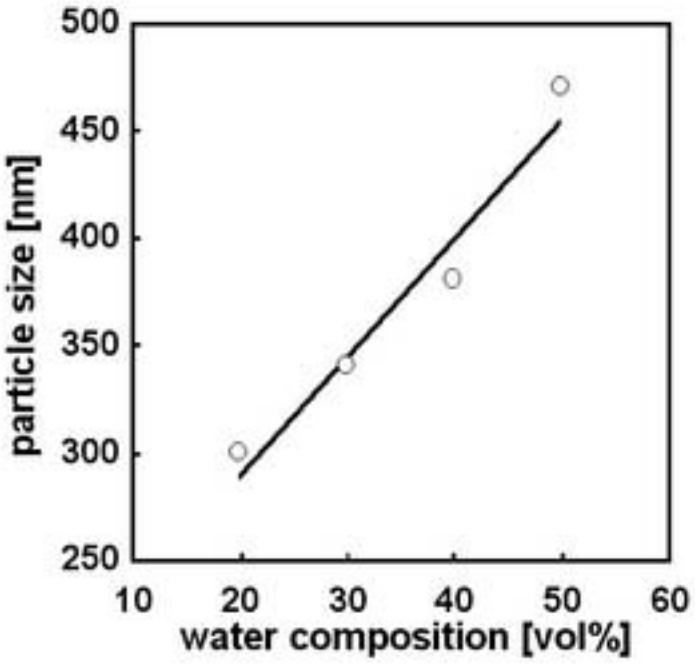

Figure 2 Hamada et al.

Figure(s)

Click here to download high resolution image

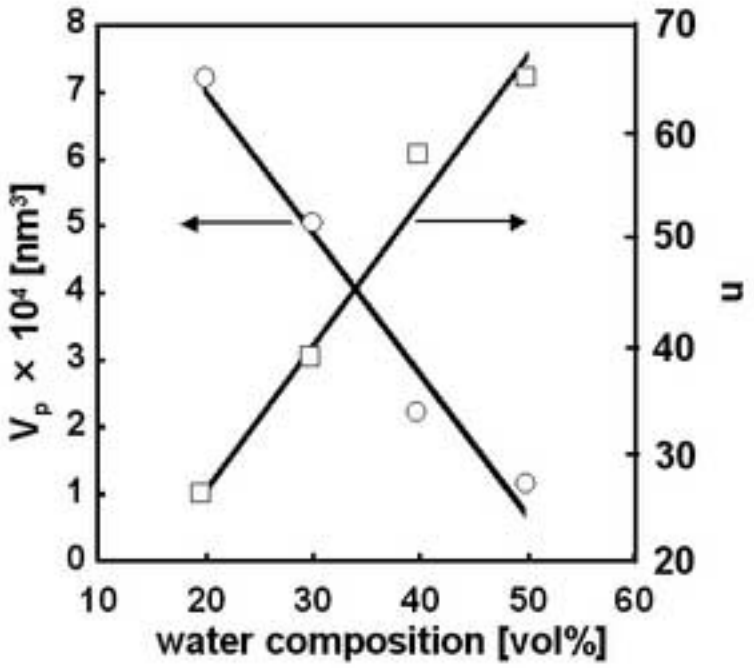

Figure 3 Hamada et al.

Figure(s)
Click here to download high resolution image

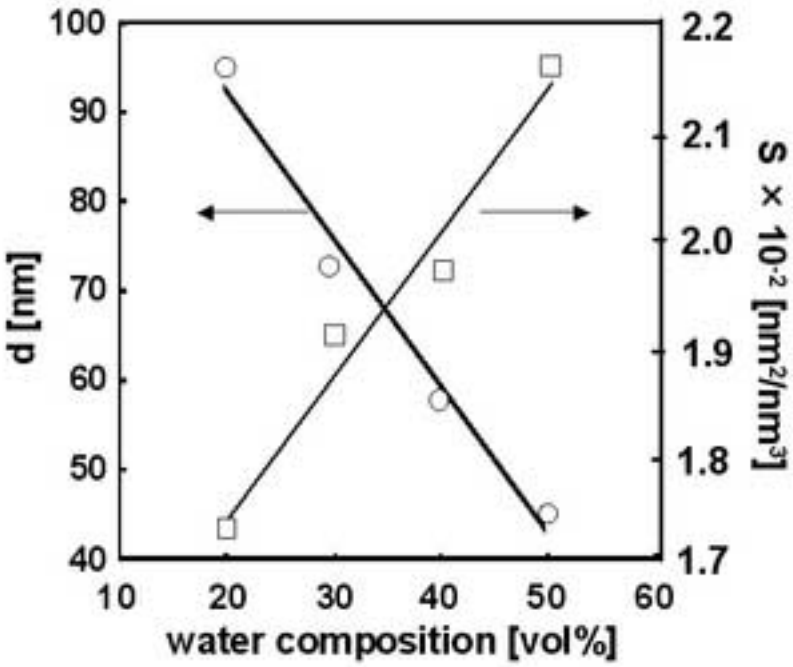

Figure 4 Hamada et al.

Figure(s)

Click here to download high resolution image

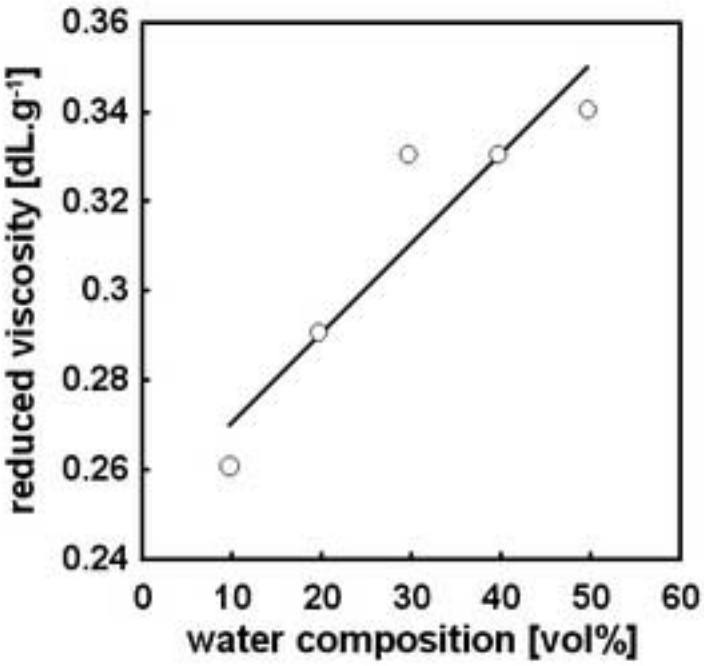

Figure 5 Hamada et al.

Figure(s)

Click here to download high resolution image

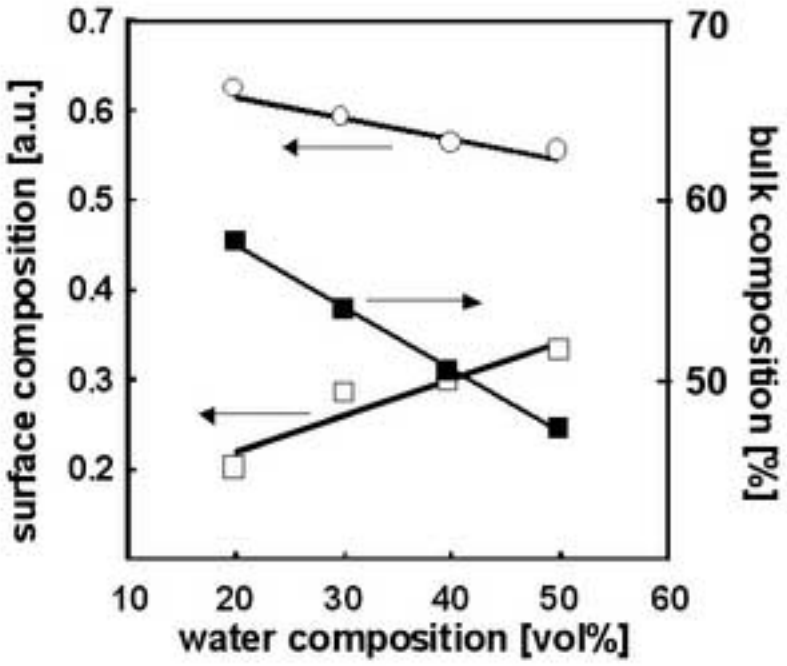

Figure 6 Hamada et al.

Figure(s)

Click here to download high resolution image

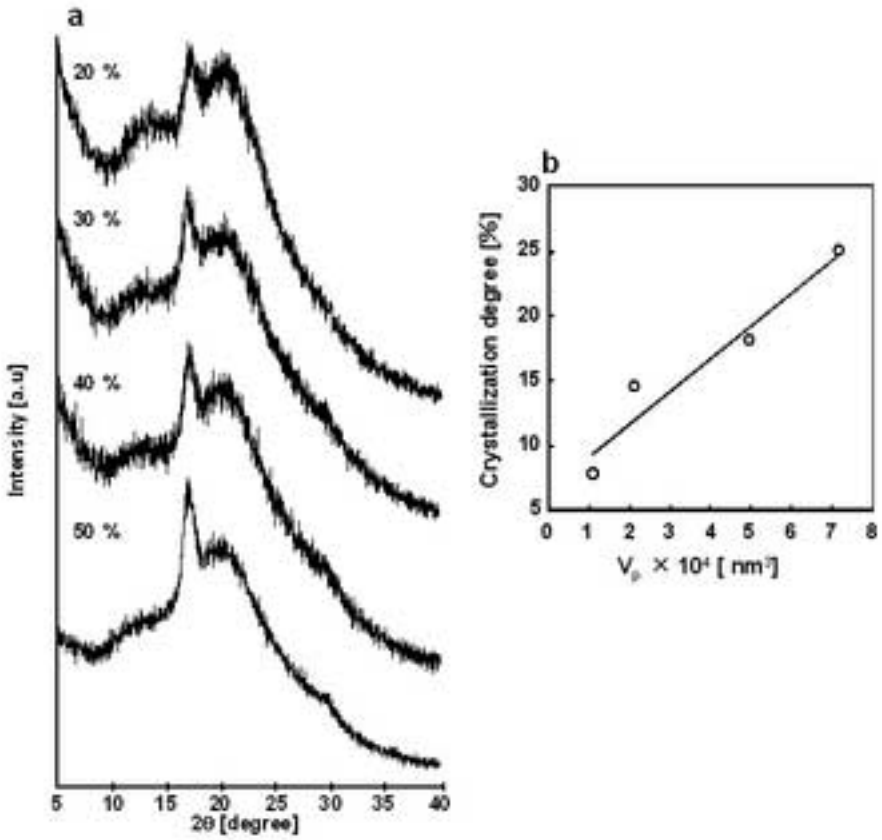

Figure 7 Hamada et al.

Figure(s)

Click here to download high resolution image

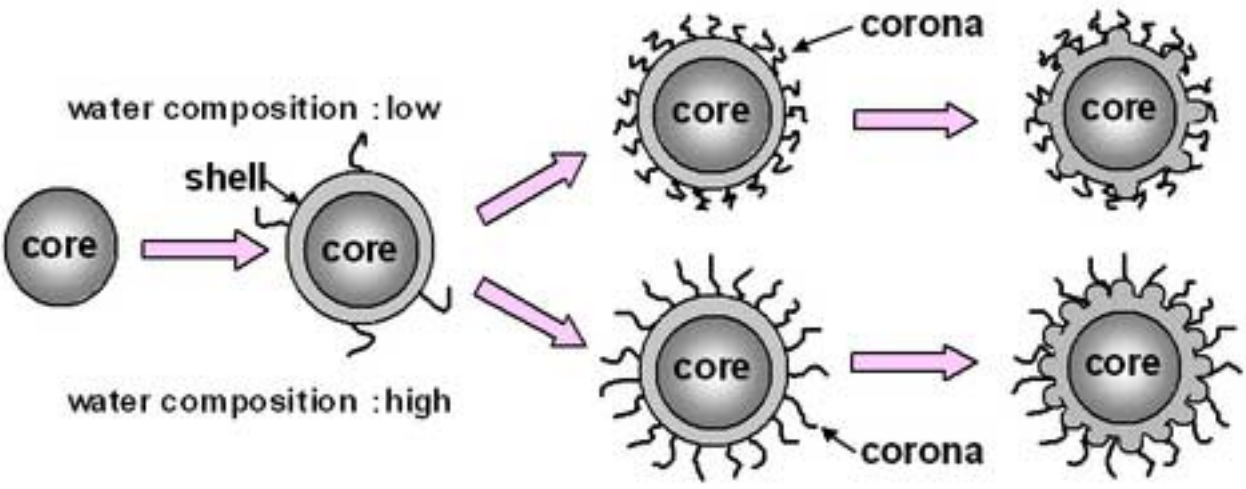

Figure 8 Hamada et al.

Figure(s)

Click here to download high resolution image

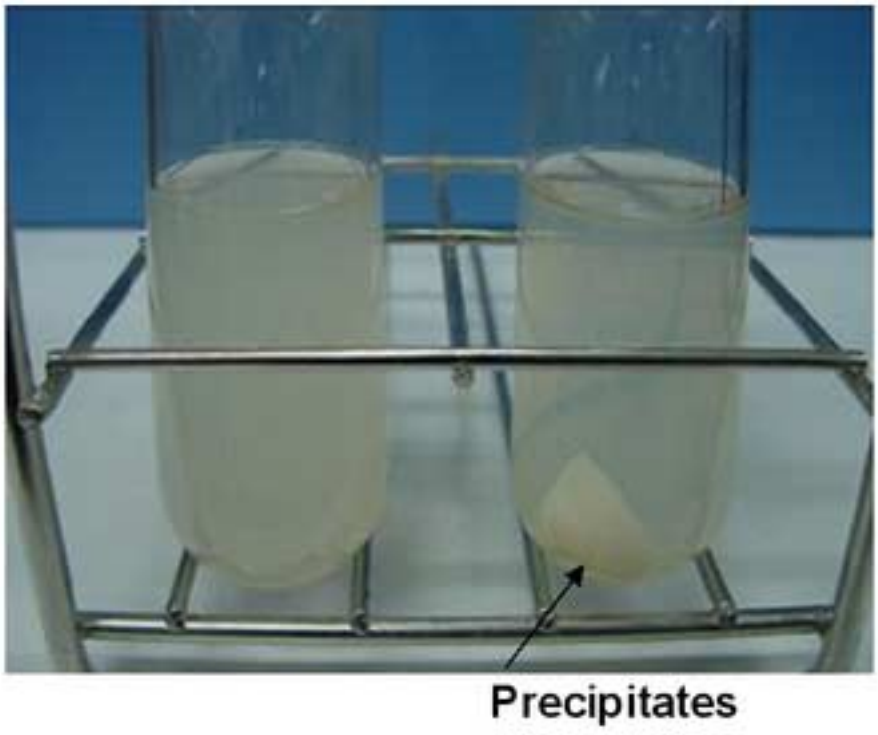

Figure 9 Hamada et al.

Table(s)

Table 1. Synthesis and Characterization of Poly(St-*co*-AN-*co*-PEGm) with Various Solvent Compositions[a]

Run	PEGm M_n	PEGm (mmol)	St (mmol)	AN (mmol)	Solvent water/ethanol = (v/v)	Composition ratio St : An : PEGm (%)
1	1740	0.027	0.9	3.0	10/90	41.5 : 58.2 : 0.3
2	1740	0.027	0.9	3.0	20/80	42.1 : 57.6 : 0.3
3	1740	0.027	0.9	3.0	30/70	45.8 : 53.9 : 0.3
4	1740	0.027	0.9	3.0	40/60	49.5 : 50.3 : 0.2
5	1740	0.027	0.9	3.0	50/50	52.5 : 47.3 : 0.2
6	1740	0.027	0.9	3.0	60/40	53.0 : 46.9 : 0.1

[a] The polymerization was carried out in the solvent (5ml) at 60° C for 24h.

Table 1 Hamada et al.